Topology Optimization for Solving Electromagnetic Inverse Problem

Jonathan Denies
CEREM - Centre for Research in Mechatronics
2, Place du Levant
Louvain-la-Neuve, Belgium
jonathan.denies@uclouvain.be

Hamid Ben Ahmed
SATIE - Laboratory
ENS Cachan Bretagne,
CNRS, UEB,
Avenue Robert Schuman,
Campus de Ker Lann,
35170, Bruz, France
benahmed@bretagne.ens-cachan.fr

Bruno Dehez
CEREM - Centre for Research in Mechatronics
2, Place du Levant
Louvain-la-Neuve, Belgium
bruno.dehez@uclouvain.be

ABSTRACT

This paper deals with solving inverse problem in the electromagnetic domain of defects detection. It proposes a general approach of the application studied with metaheuristic algorithm using topology optimization tool. The paper aims to show the capacity and the particularity of this approach applied on solving inverse problem.

1. INTRODUCTION

In several domains of technology, the quality of material used to compose device is measured to limit all risk of dysfunction. Non destructive sensors have been developed in this aim of quality testing. Now, sensors are able to create analog or digital signatures of the defects in the material.

Depending on the case of application, there are several methods to obtained signatures of the defects measured. Common methods of Non Destructive Testing (NDT) are :

- Dye penetrant inspection: It is a widely and a low cost method to locate surface-breaking defects in all non-porous materials. This method is based upon capillary action. A penetrant is applied on the surface, after that, this excess penetrant is removed;
- Magnetic particle: An intense magnetic wave is created inside the material and magnetic leakage are created by the presence of surface defects. Projection of particles on the surface reveal the presence of defects by an non-homogeneous of their distribution;
- Ultrasonic: Ultrasonic pulse-wave are launched into the test object and the sensor measure the echo;
- Radiographic: As medical imaging, a short wavelength electromagnetic radiation is used to penetrate the test object. This flux is attenuated in function of material characteristics of object meet on his way;
- Eddy-current testing: A transmitter emits a variable magnetic field to excite the test object where electromagnetic induction are used to detect defects inside the test object.

The main problem with these informations is recomposing original defects responsible of these signatures. The recomposition of original defects inside the test object is a part of the field of inverse problem that several mathematical methods are used to solve. Refer to [1, 5] for a good overview of the field, and more technical issues.

As some inverse problem methods, topology optimization tools have been developed to research the best topology inside a physical space through a material description. Their capacity to be free of the application can be use to solve inverse problem. In this paper, we present an application of electromagnetic inverse problem solved by a topology optimization tool.

2. TOPOLOGY OPTIMIZATION

The aim of the topology optimization is finding the topology of an object in terms of material distribution inside a design space. Figure 1 shows two examples of different topology based on the distribution of iron, air and copper in a 2D design space.

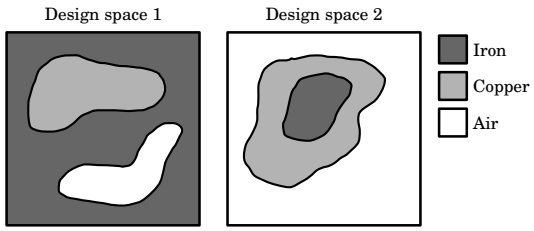

Figure 1: Example of different topology with three material distributed in a 2D design space

topology optimization is performed by a topology optimization tool consisting of three different modules (Fig. 2): an

NCMIP 2011, May 25, Paris, France

DOI 10.4108/icst.valuetools.2011.245861

optimization algorithm, a material distribution formalism and an evaluation tool.

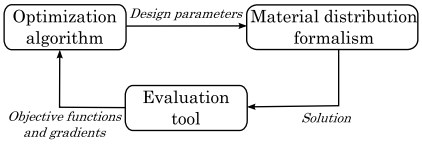

Figure 2: Interaction of three modules composing the topology optimization tool

The topology description of a solution is performed by the *material distribution formalism* with a set of design parameters. This construction follows some rules defined by the formalism. Afterthat, a numerical model is created and evaluated by the *evaluation tool*. The evaluation consist in calculating the performance of the solution. This evaluation is used by the *optimization algorithm* in order to change value of design parameters. The process iterates up to an end condition.

The three next sections describe each module composing the tool used to the study of the inverse problem. A lighter version of the tool is first presented. We call it the classical version. From this version, an advanced tool is proposed to illustrate possibility of some evolutions.

Evolution of the tool consist in developing it in taking into account the graphical aspect of the solution. Results from electromagnetic devices optimization already gives good satisfactions [2, 3, 4].

In this paper, the classical version is composed by a genetic algorithm for the optimization algorithm, a Voronoï diagram formalism for the material distribution formalism and combination of Matlab/Comsol for the evaluation tool. And the advanced version use the graphical aspect of the problem to improve reproduction tool [6, 7, 8].

2.1 Genetic algorithm

Genetic algorithm is a well-know metaheuristic algorithm in the optimization domain. It is based on the evolving of a population of individuals in a restrictive environment as follow Darwin's law. The evolution of a population is the result of reproduction of best adapted individuals.

The algorithm used this concept of evolution of a population in considering an individual by a solution, the population by a set of N_s solutions and a generation by an iteration.

Each solution i at the n^{th} generation is described by a vector of design parameters $\vec{X}_i^{(n)}$ (1) composed by D discrete variables and $N-D$ continuous variables. The concatenation of all vectors create the matrix representation of the population $\mathbf{X}^{(n)}$.

$$\vec{X}_i^{(n)} = \left\{ x_{i,1}^{(n)}, \ldots, x_{i,D}^{(n)}, x_{i,D+1}^{(n)}, \ldots, x_{i,N}^{(n)} \right\} \qquad (1)$$

Each iteration is broken down into three main part (Figure 3) to improve the main population $\mathbf{X}^{(n)}$.

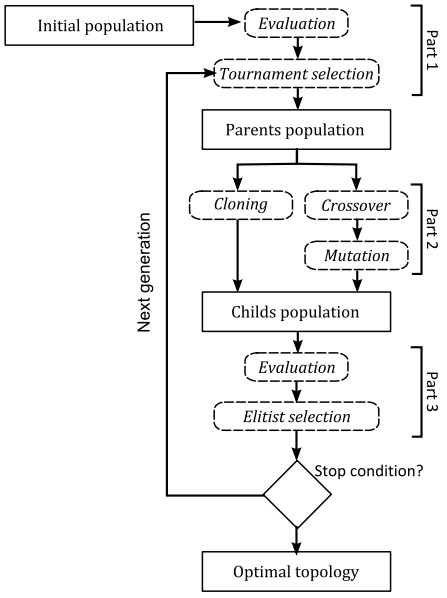

Figure 3: Diagram of the genetic algorithm

The evolution of each solution is based on the experience of old solution, through the genetic, and on some alteration on the chromosome. On first part, the algorithm compose randomly two set of potential parents: parents 1, ${}_{p1}\mathbf{X}^{(n)'}$, and parents 2, ${}_{p2}\mathbf{X}^{(n)'}$. A parent may be used several times. These parents represent the genetic bank data at the n^{th} generation.

On the second part, the i^{th} individual of the population of children, $\mathbf{X}^{(n)''}$, is a genetic combination and alteration from the i^{th} parent 1 and parent 2.

Before the third part, the population is composed by $2 \times N_s$ individuals but the main population must only be composed by N_s individuals. The aim of the third section is composing the new main population, $\mathbf{X}^{(n+1)}$, by a selection. All non-selected solutions are deleted.

In order to simplify all notations, we consider each variable at the n^{th} generation except if specified.

2.1.1 Part 1: Selection of parents

Selection of parents consists in selecting the most promising individuals by a tournament method while living some diversity. Two vectors $\vec{u}$ and $\vec{v}$ with a length of N_s elements are randomly created using a discreet uniform law $U_d(0, N_s)$. These vectors are the reference of solution inside the main population. The individual $\vec{X}_i'$ is created by copy of the best individual from the comparison of the individuals referenced by u_i and v_i.

2.1.2 Part 2: Reproduction step

The reproduction consists in a combination of cloning, crossover and mutation operation. In our case, we have decomposed the reproduction step into two branches. The first branch is a cloning of population of parents, ${}_{cl}\mathbf{X}'' = \mathbf{X}'$. We can also use the main population in the cloning step instead of the

population of parents, ${}_{cl}\mathbf{X}'' = \mathbf{X}$.

Children from the second brach are created by crossover and altered by mutation. For each child, $\vec{X}_i'$, two parents are randomly chosen inside the population of parents. The crossover operation is performed with a probability p_c.

$$ {}_{cr}X_i'' = \begin{cases} Crossover\,(X_r', X_s') & \text{If } R_i < p_c \\ Copy\,(X_r' \text{ or } X_s') & \text{If } R_i \geq p_c \end{cases} \quad (2) $$

with $R_i \sim U_c\,(0,1)$. To performs the crossover, a binary random mask is created, $\vec{m} \in \mathbb{1}^N$, in order to specify which parts from parent 1 and parent 2 will be combined. If parent 1 and parent 2 are respectively noted $\vec{X}_r' : \{x_{r,1}, x_{r,2}, \ldots x_{r,N}\}$ and $\vec{X}_s' : \{x_{s,1}, x_{s,2}, \ldots x_{s,N}\}$, the crossover operation can be write as :

$$ Crossover :_{cr} x_{i,k} = \begin{cases} x_{r,k} & \text{If } m_k = 0 \\ x_{s,k} & \text{If } m_k = 1 \end{cases} \quad (3) $$
$$ \text{with } k = 1, 2, \ldots, N $$

After, the mutation is used to inject some diversity. For each solution ${}_{cr}\vec{X}_i''$, variables ${}_{cr}x_{i,k}$ have a probability of p_m to change:

$$ Mutation :_{mu} x_{i,k} = \begin{cases} {}_{cr}x_{i,k} & \text{If } r_k < p_m \\ \alpha_k & \text{If } r_k > p_m \end{cases} \quad (4) $$
$$ \text{with } k = 1, 2, \ldots, N $$

where α_k is a random value depending of k. If $k \leq D$ then $\alpha_k \sim U_d\,(min, max)$ else $\alpha_k \sim U_c\,(0,1)$.

2.1.3 Part 3: Selection for descendants

Part 3 selects only N_s best solutions to compose a population of descendant. Then, this population is used for the next generation, $\mathbf{X}^{(n+1)}$.

2.2 Material distribution formalism

The parametrical description of a solution need to use a formalism to convert design parameters to a drawing in the design space. This is the role of the material distribution formalism. In our case, we use Voronoï diagram [9] to discretize the design space (Figure 4).

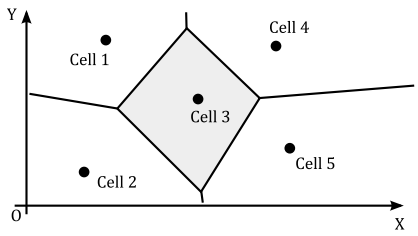

Figure 4: Diagram of the genetic algorithm

The discretization of the design space is controlled by the presence of reference points, also called Voronoï centers. Each cell is associated to a Voronoï center and represent all material point from the design space closest to the Voronoï center. To perform the material distribution, a material is associated to each cell and the Voronoï diagram is bounded to a close square normalized (Figure 5).

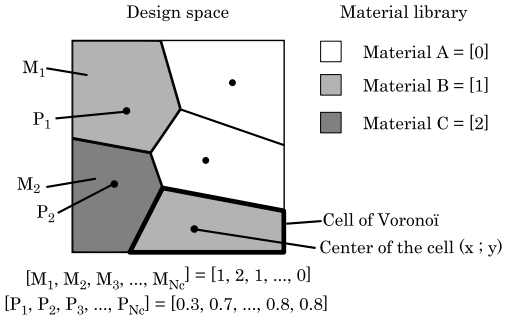

Figure 5: Example of a material distribution with Voronoï diagram coupled with three materials in reference

With this formalism, we need to use $2N_c$ continuous variables, $\vec{P} \in \Re_{\{0;1\}}^{2N_c}$, and N_c discrete variables, $\vec{M} \in \mathbb{Z}^{N_c+}$, to respectively describes the position of the Voronoï center and material center of N_c cells as illustrated in Figure 5. All parameters are merged to one vector :

$$ \{m_{i,1}, \ldots, m_{i,N_c}, x_{i,1}, \ldots, x_{i,N_c}, y_{i,1}, \ldots, y_{i,N_c}\} \quad (5) $$

With the graphical representation, we can modified the crossover operation and mutation operation. Instead of change chromosome and observe the modification inside the design space, it is possible to change directly inside the design space and observe the impact on the chromosome.

The graphical crossover operation uses a graphical pivot to divide the design space into two regions to switch. At each operation, a random circle $\mathscr{C}\,(x, y, r)$ is defined to subdivide the design space into two regions: inside $\mathscr{D}$ and outside $\mathscr{O}$ the circle. All Voronoï cells are associated to a region in function of the position of their reference point. A binary mask vector, $\vec{m} \in \mathbb{1}^{N_c}$, is used to represent which cell is associated to the inside or outside region. If $P_k \in \mathscr{D}$ then $m_k = 1$ else $m_k = 0$ for the first parent and the procedure is reversed for the second parent.

Finally, all Voronoï centers with $m_k = 1$ from both parents are copied to create the child solution with now N_c' cells (Figure 6).

The graphical mutation consists in considering the displacement of a Voronoï center as a graphical local deformation. The displacement can be write as a choice of a distance r and an angle θ (Figure 7). The distance r is decomposed on a random term $\epsilon \sim U_c\,(0,1)$ and a factor of proportionality term α.

The value of the factor of proportionality α depend on the neighborhood of each Voronoï cell. The value is chosen to be the half of the distance of the nearest Voronoï cell. We

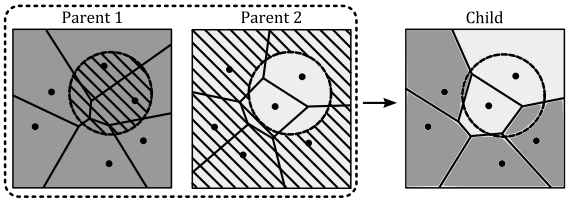

Figure 6: Example of a graphical crossover with a circle

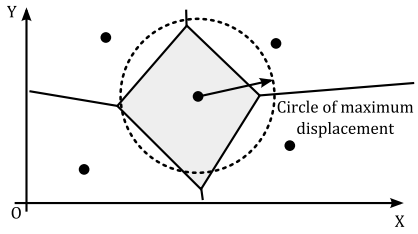

Figure 7: Illustration of a local displacement of a Voronoï center

can write the mutation on the x- and y-coordinate of the Voronoï center in a decomposition of cosine and sine part:

$$\begin{array}{ll} \text{x-coordinate :} & {}_{mu}x'_{i,k} = {}_{cr}x'_{i,k} + \alpha\epsilon cos\,(\theta) \\ \text{y-coordinate :} & {}_{mu}y'_{i,k} = {}_{cr}y'_{i,k} + \alpha\epsilon sin\,(\theta) \end{array} \quad (6)$$

If the parameter ${}_{mu}x'_{i,k}$ lifted out the design space with a distance Δ from the edge, a new value is attributed. If ${}_{mu}x'_{i,k} > 1$ then ${}_{mu}x'_{i,k} = 1 - \Delta$ else if ${}_{mu}x'_{i,k} < 0$ then ${}_{mu}x'_{i,k} = \Delta$. We perform same work for ${}_{mu}y'_{i,k}$ parameter.

2.3 Evaluation tool

The evaluation tool is composed by a combination of Matlab and Comsol softwares. All material distributions proposed by the material distribution formalism are solved and evaluated by finite-elements.

To maintain the real solution proposed by the tool, we choice to create an adapted mesh for each solution. With this method, this is not the solution adapting itself to the mesh, but the mesh that adapt itself to the solution in order to not modify the solution proposed by the optimization algorithm.

3. STUDY CASE

An electromagnetic sensor is used to test the quality of an iron object, i.e. in our case an iron bar. The sensor is powered by a AC current and must move along the surface in order to obtain the signature of defects. In our study, the problem is limited to a static 2D problem with no magnetic saturation, powered by a DC current, the sensor do not move, and we measure only the magnetic field inside the bar. Figure 8 shows the device and the test object. This simplification do not change the global approach by topological optimization but reduced the cost time for the evaluation of each solution. Each evaluation cost 4 seconds on a 3Ghz computer. A most realistic case will be studied later.

Target defects to retrieve are illustrated on Figure 9 with

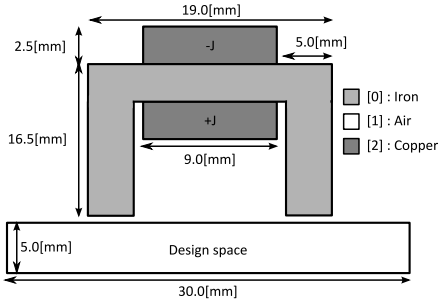

Figure 8: Sheme of the study case, the electromagnetic sensor and the test object

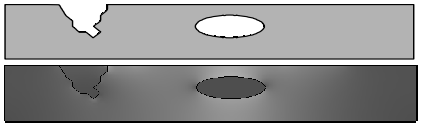

Figure 9: Target topology and magnetic flux density field associated

the magnetic flux density field normalized (the figure draws only the design space).

The objective is minimizing the relative error between target magnetic flux density field normalized, $\mathbf{B}_{i,j}$, and proposed magnetic flux density field normalized, $\mathbf{B}'_{i,j}$, with $\mathbf{B}_{i,j} = \sqrt{\mathbf{B}_x^2\,(x_i, y_j) + \mathbf{B}_y^2\,(x_i, y_j)}$, and (x_i, y_j) are points inside the design space:

$$\min\left(\sum_{i=1}^{50}\sum_{j=1}^{50}\left|\frac{\mathbf{B}_{i,j} - \mathbf{B}'_{i,j}}{\mathbf{B}_{i,j}}\right|^2\right) \quad (7)$$

4. RESULTS AND DISCUSSIONS

Since the algorithm use probabilities laws to improve solutions, five runs are executed to represent the variance of the final result. All runs stage a population of $N_s = 10$ solutions during $n_{max} = 500$ generations. Crossover and mutation probability are fixed to 90% and $1/N_c$. The number of cells is initially set to 60.

Figure 10 shows the convergence and the variance of the best solution during the optimization process. The global research is fast but finally fall in a local optimum. A final design is showed on Figure 11.

All final topologies from the five runs are identical as the target topology but not the shape. The oval is found but not really the crack.

The choice of $N_s = 10$ may be discussed. To improve the global exploration in the solutions space, the value of N_s may be higher. However, the number of generations must be decreased to conserve the relation $I = N_s \times n_{max}$, where I is the number of evaluations used by the tool. In our case, we want to study the capacity of the algorithm to approach graphical details. To improve performance, another possible approach would be to use a high value for N_s and decline its

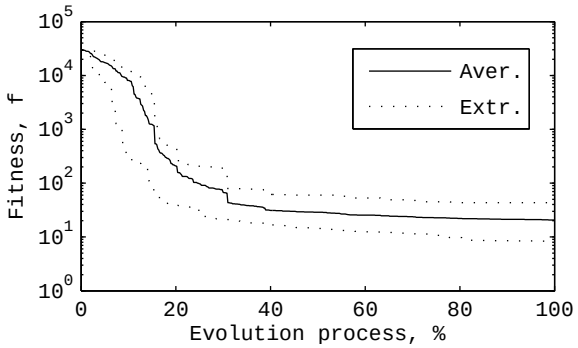

Figure 10: Convergence of run with variance for 5 runs

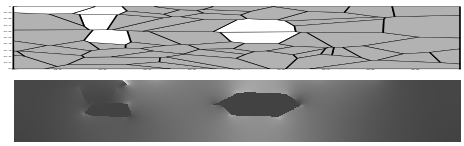

Figure 11: Final design and magnetic flux density field associated

value over the iterations. With this last proposition, we can combine exploration in the beginning of the optimization and intensification in the end of the optimization.

The choice of the value of p_m may also be discussed. Generally, the diversity must be low at each generation in order to give some diversity for the crossover. We consider that a value near of one mutation ($p_m = {}^1/_{N_c}$) by solution by iteration is adequate. However, it is also possible to give a high value in the beginning of the process to decrease to a lower value.

5. CONCLUSIONS

The aim of this paper is to present an original approach to solve inverse problem when the problem is an ill-posed problem. Despite the time-computing required to obtain the final solution, final designs obtained greatly resemble the target solution.

Both alternatives proposed for genetic algorithm parameters, N_s and p_m, of the genetic algorithm are currently in studies in order to improve the exploration in the beginning of the optimization and the intensification in the end of the optimization.

Acknowledgment

J. Denies is funded by a Belgian F.R.I.A grant.

6. REFERENCES

[1] J. Bowler and D. Lesselier. *editors. Inverse problems 2002 18*, pages 1733–1963, 2002.

[2] J. Denies, H. B. Ahmed, and B. Dehez. Design of a ferrofluid micropump using a topology optimization method. In *Proceedings of the Electromotion 2009 Conference, Lille, France*, July 2009.

[3] J. Denies, H. B. Ahmed, B. Dehez, and F. Glineur. Topology optimization with hybrid algorithm coupled to voronoï formalism. In *19th International Conference on Electrical Machines, ICEM'10, Roma, Italy*, September 2010.

[4] J. Denies, B. Dehez, and H. B. Ahmed. Simulated annealing and genetic algorithms in topology optimization tools : a comparison through the design of a switched reluctance machine. In *Proceedings of the International Symposium on Power Electronics, Electrical Drives, Automation and Motion - Speedam 2010, Pisa, Italy*, pages 1247–1252. IEEE Press, Juny 2010.

[5] N. Ida. Numerical modelling for electromagnetic non-destructive evaluation. *London: Chapman and Hall*, 1995.

[6] E. Jensen. *Topological structural design using genetic algorithms*. PhD thesis, Purdue University, November 1992.

[7] C. Kane. *Algorithmes génétiques et optimisation topologiques de formes*. PhD thesis, Ecole Polytechnique, September 1995.

[8] C. Kane and M. Schoenauer. Genetic operators for two-dimensionnal shape optimization. *Artificial Evolution, Springer*, pages 355–369, 1996.

[9] S. S. Skiena. Voronoi diagrams. *§8.6.4 in The Algorithm Design Manual. New York: Springer-Verlag*, pages 358–360, 1997.